Pan-transcriptome-based Candidate Therapeutic Discovery for Idiopathic Pulmonary Fibrosis

Yunguan Wang[1], Jaswanth K. Yella[1,2], Sudhir Ghandikota[1,2], Tejaswini C. Cherukuri[3], Satish K. Madala[3,4], Anil G. Jegga[1,2, 4,*]

[1]Division of Biomedical Informatics, Cincinnati Children's Hospital Medical Center, Cincinnati, .Ohio, USA

[2]Department of Computer Science, University of Cincinnati College of Engineering, Cincinnati, Ohio, USA

[3]Division of Pulmonary Medicine, Cincinnati Children's Hospital Medical Center, Cincinnati, Ohio, USA

[4]Department of Pediatrics, University of Cincinnati College of Medicine, Cincinnati, Ohio, USA

[*]Corresponding author

Anil G. Jegga

Cincinnati Children's Hospital Medical Center

240 Albert Sabin Way, MLC 7024

Cincinnati

OH 45229

Off: 513-636-0261

Fax: 513-636-2056

Email: anil.jegga@cchmc.org

ABSTRACT

Rationale: Although the advent of two FDA-approved therapies for idiopathic pulmonary fibrosis (IPF) has energized the field, their effects are largely suppressive than pulmonary fibrosis remission- or reversion-inducing. Hence, the pursuit for newer IPF therapeutics continues. Recent studies showed that joint analysis of systems biology level information with drug-disease connectivity are effective in discovery of biologically-relevant candidate therapeutics.

Objectives: To identify novel candidate therapeutics for IPF

Methods and Measurements: Publicly available gene expression signatures from IPF patients are used to query large scale perturbagen signature libraries to identify compounds that can potentially reverse IPF. Two methods are used to calculate IPF-compound connectivity: gene expression-based and feature-based connectivity. Identified compounds are further prioritized based on shared compound mechanisms of action.

Results: We identified 77 compounds as potential candidate therapeutics for IPF. Of these 39 compounds are either FDA-approved for other diseases or are currently phase 2/3 trial drugs suggesting their repurposing potential for IPF. Among these compounds are multiple receptor kinase inhibitors (e.g., nintedanib, currently approved for IPF, and sunitinib), aurora kinase inhibitor (barasertib), EGFR inhibitors (erlotinib, gefitinib), calcium channel blocker (verapamil), phosphodiesterase inhibitors (roflumilast, sildenafil), PPAR agonists (pioglitazone), HDAC inhibitors (entinostat), and opioid receptor antagonists (nalbuphine).

Conclusion: As almost half of the candidates we have discovered in this study are either FDA-approved or are currently in clinical trials for other diseases, rapid translation of these

compounds is potentially feasible. The generalizable, integrative connectivity analysis framework in this study can be readily adapted in early phase drug discovery for other diseases.

Introduction

Idiopathic pulmonary fibrosis (IPF), a chronic and fatal fibrotic lung disease in people over 50 years old is estimated to affect 14 to 42.7 per 100,000 people (1). IPF is characterized by progressive subpleural and paraseptal fibrosis, heterogeneous honeycomb cysts (honeycombing), and clusters of fibroblasts and myofibroblasts (2). The median survival time of patients with IPF is 2.5 to 3.5 years, with 5-year survival rate around 20% (1). Currently, two small molecules - pirfenidone and nintedanib - are approved for IPF and are reported to slow down lung function decline caused by disease progression. However, drug induced side-effect profiles of these two drugs are formidable and their therapeutic effects are suppressive rather than pulmonary fibrosis remission or reversal (3, 4). The pursuit of relatively safer and efficacious therapies or combinatorials that arrest, or reverse fibrosis therefore continues. On the other hand, technological advances in experimental and computational biology resulted in rapidly expanding genomic and biomedical data, including transcriptomic profiles of disease and small molecules, disease or drug associated pathways and protein-protein interactions (5-7). Various approaches have been developed to facilitate *in silico* drug discovery via joint analysis of these data including the connectivity mapping-based method, a widely used approach (8).

The concept of connectivity mapping between a drug and a disease is defined as the gene expression-based similarity calculated using a Kolmogorov-Smirnov statistic like algorithm (9, 10). It was first introduced as the ConnectivityMap (CMap) and succeeded by the LINCS L1000 project and the CLUE platform (8, 11), which currently contain gene expression profiles of ~20,000 small molecule perturbagens analyzed in up to 72 cell lines. The connectivity mapping

concept and application have led to the discovery of novel candidate compounds for disease, drug repurposing candidates, and novel drug mechanism of actions (12-16).

Recently similar efforts - *in silico* drug discovery for IPF – have been reported wherein joint analysis of systems biology level information with drug-IPF connectivity are used to discover biologically relevant candidate therapeutics for IPF. For instance, Karatzas et al developed a scoring formula to evaluate drug-IPF connectivity obtained from multiple sources and identified several IPF candidate therapeutics (17). Interestingly, neither of the two approved IPF drugs (pirfenidone and nintedanib) was re-discovered by their approach (17). In another recent study using network-based approach and integrated KEGG network with connectivity analysis sunitinib, dabrafenib and nilotinib were identified as potential repurposing candidates for IPF (18). Interestingly, the network-based approach was able to re-discover nintedanib. However, the application of this is potentially limited because the construction of the network is based on KEGG pathways and known drug targets only.

Using a similar approach, namely, by examining connectivity between IPF gene signature and LINCS small molecules, we discovered 17-AAG (a known Hsp90 inhibitor) as a potential candidate therapeutic that inhibits fibroblast activation in a mouse model of pulmonary fibrosis (14). In another related study, we screened connectivity of LINCS small molecules with cystic fibrosis (CF) and integrated systems biology level information from CFTR to identify a candidate drug for cystic fibrosis (13). These results suggest that disease-drug connectivity complemented with systems biology level information of drugs and disease could facilitate more

accurate candidate discovery. In this study we therefore calculated both gene-expression and enriched-pathway based connectivity between IPF and small molecules in an unsupervised manner and integrated these results with cheminformatic knowledge to prioritize candidate therapeutics for IPF. We have identified 77 (out of ~20,000 LINCS small molecules) candidate therapeutics for IPF. Significantly, among these were the approved drug for IPF (nintedanib), as well as several others that are either currently being investigated or reported as a potential candidate therapeutics for IPF (sunitinib and nilotinib). This suggests that the current approach has the potential to identify "true" candidate thereapeutics. Recent in vitro and in vivo preclinical studies have reported beneficial effects of HDAC inhibitors (HDACIs) in preventing or reversing fibrogenesis (19, 20). Further, there are currently four HDACIs approved by the US FDA for cancer treatment but none for fibrotic diseases. Therefore, in the current study, we have selected entinostat (MS-275 or SNDX-275), a class-I HDACI, from our computational screening results for *in vitro* validation.

Methods

Cohort selection

We used publicly available gene expression profiles from the Gene Expression Omnibus (GEO) (21) database as a basis for generating IPF gene expression signatures. Since gene expression profiles are known to be heterogeneous in different patients (22, 23), we selected 6 GEO datasets comparing primary healthy human lung tissues with primary IPF lung tissues for this study to potentially mitigate such heterogeneity (Table 1).

Differential analysis of IPF gene expression profiles

Differential analysis was performed in R in using the package "limma" (24). Genes with fold change above or equal to 1.5 and adjusted p-value less than or equal to 0.05 were considered differentially expressed. Each dataset was analyzed separately.

IPF-compound connectivity estimation and permutation analysis

To correct for multiple testing problem introduced by conducting connectivity analysis in multiple datasets, we used permutation analysis to estimate the significance of connectivity. First, we constructed a matrix of connectivity score, denoted by *s*, between CLUE compound ***i*** and IPF dataset ***d*** in cell line ***j***. Next, positive and negative connectivity to IPF were determined by thresholding connectivity score at 90 and -90, respectively:

$$c_{i,d,j} = \begin{cases} 1, & (s_{i,d,j} \geq 90) \\ 0, & (-90 < s_{i,d,j} < 90) \\ -1, & (s_{i,d,j} \leq -90) \end{cases}$$

Overall connectivity, denoted by *o*, between each compound to IPF across all cell lines is summarized as the sum of individual connectivity across all datasets and all cell lines:

$$o_i = \sum_{d}^{m} \sum_{j}^{n} c_{i,d,j}$$

Permutation was performed by randomly shuffling rows of the connectivity matrix **C**, so that compound names were randomly assigned. Then, the permutated overall compound-to-IPF connectivity **O'** scores were calculated, and we recorded incidences where $o_i \leq o_i$', which indicates the observed compound to IPF connectivity is not larger than random connectivity:

$$f_{ip} = \begin{cases} 1, & (o_i \leq o_i') \\ 0, & (otherwise) \end{cases}$$

We repeated the permutation tests for 100,000 times and estimated significance as the frequency of **F** overall all permutations. Significance cut-off was set at 0.05.

Functional enrichment

Functional enrichment analysis was performed using the pre-compiled libraries from the ToppGene Suite (25). Enrichment p values were calculated using hypergeometric test in Python using the scipy package.

Annotation-based connectivity analysis

Annotation-based compound-IPF connectivity was generated and evaluated as follows:

(1) Identify enriched annotation terms enriched in conserved IPF genes (genes that were dysregulated in more than 4 IPF datasets) via functional enrichment analysis, resulting in two vectors, $\boldsymbol{I_{up}}$ and $\boldsymbol{I_{down}}$;

(2) Calculate enrichment score,$\boldsymbol{P_{i,up}}$ and $\boldsymbol{P_{i,down}}$, of the 500 highest and lowest expressed genes of each LINCS L1000 small molecule expression profile, denoted by **i**, in the up-regulated and down-regulated IPF pathways identified in step (1);

(3) Calculate annotation-based connectivity score, defined as Pearson correlation between $\boldsymbol{P_{i,up}}$ and $\boldsymbol{I_{down}}$, and between $\boldsymbol{P_{i,down}}$ and $\boldsymbol{I_{up}}$;

(4) To correct false positives from multiple testing, permutation analysis were performed by swapping annotation terms in $\boldsymbol{P}_{i,down}$ and $\boldsymbol{P}_{i,up}$, followed up recalculation of annotation-based connectivity. 100,000 permutations were performed with significance threshold set to 0.05.

Primary lung fibroblast cultures and RT-PCR. Lung lobes from TGFα mice on Dox for four weeks were collected in Iscove's Modified Dulbecco's Medium containing 5% FBS (Life Technologies, NY, USA). Lung pieces were finely minced with sterile razor blades into 5ml of Dulbecco's Modified Eagle's Medium (Life Technologies, NY, USA) containing collagenase (2mg/ml) and incubated at 37°C for 30min for tissue digestion. Digested tissue was passed through a 100 µm filter, washed twice with Iscove's medium, plated onto 100 mm tissue-culture plates, and incubated at 37°C, 5% CO_2 to allow cells to adhere and migrate away from larger remaining tissue pieces. Unbound cells were removed on Day 3 of culture, and cells were fed with fresh Iscove's medium. Adherent primary lung fibroblasts were harvested on Day 5 or 8 for drug treatment studies. After drug treatments, total RNA was extracted using RNAeasy Mini Kit (Qiagen Sciences, Valencia, CA, USA) and RT-PCR assays were performed. Relative quantities of mRNA for several genes were determined using SYBR Green PCR Master Mix (Applied Biosystems) and target gene transcripts in each sample were normalized to hypoxanthine guanine phosphoribosyl transferase (HPRT) and expressed as a relative increase or decrease compared with controls. RT-PCR Primer sequences for genes, HPRT (Fwd, CCCTTGACTATAATGAGTACTTCAGG; Rev, TTCAACTTGCGCTCATCTTAGG), CCNA2 (Fwd, CTTGGCTGCACCAACAGTAA; Rev, CAAACTCAGTTCTCCCAAAAACA), CCNB2 (Fwd, CAACCGTACCAAGTTCATCG; Rev, GAGGGATCGTGCTGATCTTC), αSMA (Fwd, TGACGCTGAAGTATCCGATAGA; Rev, CGAAGCTCGTTATAGAAAGAGTGG) and

KIF20A (Fwd, AAGGACCTGTTGTCAGACTGCT; Rev, TGAGGTGTCCTCCAGTAGAGC).

Result

Differential expression analysis of IPF datasets

We analyzed 6 gene expression datasets comparing gene expression between lung tissue derived from IPF patients and those from healthy controls (Table 1). Differential expression analysis was performed in each dataset using the R package "Limma". Differentially expressed genes (DEG) were defined as genes with fold change above or equal to 1.5 and FDR-BH adjusted p-value less than or equal to 0.05. The number of DEGs ranged from 263 to 2385, and 4677 genes were unambiguously up-regulated, and 2210 genes were unambiguously down-regulated in at least one IPF dataset (**Figure 2a; Supplementary Table 1)**. Overall similarity between DEG gene lists is low, as is reflected by the median Jaccard index between gene lists of only 0.077. The large discrepancy between datasets suggests disease heterogeneity in IPF but also justifies performing meta-analysis across multiple datasets to extract high confidence drug candidates for IPF. Despite the large heterogeneity in DEG among different IPF datasets, there were also a considerable number of genes that were consistently dysregulated in 4 or more IPF datasets, which we call the conserved IPF gene set (197 up-regulated genes and 84 down-regulated genes). Among these conserved DEGs, 60 genes were known previously to be involved in pulmonary fibrosis (**Figure 2b)**. Functional enrichment analysis of conserved IPF genes showed that biological processes involved in extracellular matrix formation, inflammation responses and cell migration were up-regulated while processes involved in normal lung processes such as angiogenesis and alveolar functions were down-regulated.

Expression based connectivity analysis and permutation analysis.

We used the NIH Library of Integrated Network-Based Cellular Signatures (LINCS) library as our search space for IPF therapeutic candidates. The LINCS library contains expression profiles of ~20,000 small molecules assayed in various cell lines. To identify potential IPF candidate therapeutics, we adopted the connectivity mapping method which assumes small molecules with gene expression profiles negatively correlated with that of a disease are likely to be therapeutic for the particular disease. We first queried the Connectivity Map web platform (CLUE.io) for compounds with a reversed gene expression profile comparing to IPF. From each dataset, a gene signature containing up to 150 most up-regulated and down-regulated genes was extracted and used to query the CLUE platform (**Figure 2c** and **Supplementary Table 2)**. Using the hits from CLUE results, we applied a "greedy" approach to capture the highest number of compounds connected to IPF by selecting compounds with at least 90 connectivity score in any one of the cell lines. This approach returned 1000+ compounds that are connected with IPF at least once. A problem with this approach is that it introduces many compounds whose connection to IPF is observed in both the directions, i.e., potentially inducing and reversing IPF gene expression profiles at the same time (**Figure 3a)**. This indicates that the gene expression perturbation due to technical variation is present in our data and is reflected in the form of these low frequency compounds in CLUE analysis. Under the assumption that IPF pathogenesis related gene expression patterns are consistently present in our selected 6 IPF datasets, we performed permutation analysis to estimate the significance of IPF-disease connectivity and filter out false positives. With a significance cut-off at 0.05, we identified 82 compounds that were significantly connected with IPF (**Figure 3b)**. These compounds were associated with 63 different mechanisms of action.

Functional enrichment-based connectivity analysis

One limitation of using the Touchstone Library based CLUE platform to screen for drug candidates is that it only covers 2,836 out of ~20,000 small molecules in the full L1000 database. To overcome this, we searched for IPF candidate therapeutics among the remaining ~17,000 LINCS small molecules. To do this, we used a functional enrichment based metric to evaluate drug-IPF connectivity of these LINCS small molecules, wherein gene expression data from both the compound and the IPF data sets were transformed into enrichment p-values using hypergeometric tests against gene functional annotations (Gene Ontology Biological Process, Mouse Phenotypes and KEGG pathways). To minimize the noise introduced by biological processes not relevant to IPF, we only considered functional annotations enriched in the conserved IPF gene sets, and thus, each compound enrichment profile was limited to these pathways. Connectivity between a compound and IPF was defined as the cosine similarity between the p-values of pathways enriched in compound up-regulated genes and those enriched in IPF down-regulated genes, and vice versa. Next, we used the same permutation analysis step as discussed in the previous sections to estimate the significance of the feature-based compound-IPF connectivity, and identified 345 compounds that perturbed IPF-related pathways in an overall opposite manner compared to IPF. In order to find groups of functional related therapeutic candidates that could act on IPF perturbed biological processes, we performed clustering analysis on the compound enrichment profiles and prioritized four clusters of compounds with high connectivity to IPF. The compounds in three clusters selectively down regulated pathways such as ‘cell adhesion’, ‘collagen metabolic process’ and ‘ regulation of programmed cell death’, which were up-regulated in IPF. On the other hand, compounds in the

remaining cluster up-regulated pathways such as 'blood vessel morphogenesis' and 'angiogenesis', which were down regulated in IPF. The approved IPF drug, nintedanib was in this cluster of compounds. Combining compounds from these four clusters, we identified 103 candidates as IPF therapeutic candidates from annotation-based connectivity analysis (**Figure 4)**. These compounds include EGFR inhibitor gefitinib, PDGFR and VEGFR inhibitor dovitinib, and KIT inhibitor sunitinib.

Prioritization of IPF candidate therapeutics based on shared mechanism of action

In the annotation-based connectivity analysis, we observed that the several of the ranked compounds shared drug mechanisms of action (MoA). For instance, EGFR inhibition, PDGFR inhibition and VEGFR inhibition were shared across multiple compounds suggesting potential relevance of these MoAs to IPF. This also suggests a likelihood of higher therapeutic potential of multiple compounds with shared and similar MoAs. Leveraging the known MoA information of the discovered compounds, we further prioritized compounds belonging to MoA that were prioritized by annotation-based connectivity analysis. After removing glucocorticoid receptor agonists and immunosuppressants from the list because of their known detrimental effects in IPF, we identified 48 MoAs meeting this criteria (**Supplementary Table 3**). Based on these MoAs, we selected 77 compounds as our final pre-clinical candidates for IPF (**Supplementary Table 4)**. Among these, 39 were FDA-approved drugs or phase-II/III compounds suggesting their repositioning potential for IPF (**Table 2)**. These drugs include Bcr-Abl kinase inhibitors, EGFR inhibitors, opioid receptor inhibitors, receptor tyrosine kinase (RTK) inhibitors and aurora kinase inhibitors. Notably, the approved IPF drug nintedanib was also among this list. This is important because Nintedanib was not included in the CLUE database, and would have been missed if

annotation-based connectivity were not examined. A closer look at the pharmacological targets of these candidates revealed that many of these targets such as PDGFRA, EGFR, FGFR4, FYN and KDR were differentially expressed in IPF. Among these targets, KDR, FGFR4 and PDGFRA are associated with nintedanib and other multi-targeted RTK inhibitors such as dovitinib, pazopanib and sunitinib (**Figure 5)**. These genes are involved in VEGF and PI3k/AKT signaling and VEGFR2 mediated cell proliferation, suggesting a role for multi-targeted RTK inhibitors in controlling IPF through VEGF signaling inhibition.

Anti-fibrotic potential of entinostat (MS-275 or SNDX-275)

Recent studies have reported the beneficial effects of HDAC inhibitors (HDACIs) in preventing or reversing fibrogenesis. For instance, HDAC8 was reported to contribute to pulmonary fibrosis and NCC170, a HDAC8-selective inhibitor, repressed TGFβ1-induced fibroblast contraction and α-SMA protein expression in normal human lung fibroblasts (19). Another study reported that vorinostat or SAHA (suberoylanilide hydroxamic acid), a known HDACI, induces apoptosis in IPF fibroblasts (20). There are currently four HDACIs approved by the US FDA for cancer treatment but none for IPF. Therefore, in the current study, we have selected entinostat (MS-275 or SNDX-275), a class-I HDACI, from our computational screening results for *in vitro* validation. Primary lung fibroblasts were isolated from fibrotic lung lesions of TGFα mice and treated with either vehicle or entinostat (Figure 6). We observed a significant reduction in the expression of fibroproliferative genes (CCNA2 and CCNB2), αSMA and KIF20A with MS 275 treatment for 48 hrs compared to vehicle treated fibroblasts (Figure 6). Together, these findings support that anti-fibrotic drugs identified using *in silico* screening methods are effective in inhibiting

fibroblast activation and may serve as potential drug candidates for further validation using both *in vitro* and *in vivo* pre-clinical IPF models.

Discussion

In this study, we developed a multiplexed, generalizable approach to discover novel therapeutics by integrating disease-driven and perturbagen-driven gene expression profiles, disease-associated biological pathways, and cheminformatics of perturbagen. Compound-IPF connectivity were examined from different dimensions including transcriptome, functional enrichment profiles, and drug mechanisms of actions. With this approach, we not only identified approved IPF therapeutic drugs (nintedanib) but also identified additional FDA-approved drugs that share similar MOA as IPF candidate therapeutics. Notably, these drugs were not discoverable using conventional transcriptome based connectivity analysis alone. Further, approved drugs or investigational compounds associated with MoAs such as Bcr-abl inhibitor and Aurora kinase inhibitor, were also among our candidate list, which could provide insights into novel intervention strategies against IPF.

Transcriptome based connectivity mapping was first introduced more than a decade ago and has been applied to facilitate drug discovery for various diseases, including IPF. In a recent study, Karatzas et al proposed nine drugs as IPF therapeutics based on their connectivity with expression profiles derived from IPF datasets. However, they were not able to re-discover approved IPF drugs although these drugs were included in the LINCS L1000 library that was queried (17). Likewise, our gene expression based connectivity approach through CLUE prioritized 82 small molecules as IPF therapeutics candidates, but neither of the FDA approved IPF drugs (pirfenidone or nintedanib) was in the list. A closer look at the connectivity scores revealed that pirfenidone had no connectivity to IPF in any of the six queried datasets, although it was connected to 2 of our prioritized IPF candidates, histamine receptor antagonist ranitidine

and calcium channel blocker verapamil. On the other hand nintedanib was not included in CLUE and thus no information regarding its connectivity to IPF could be obtained in this way.

We also examined the connectivity between the ~17,000 compounds not covered by CLUE and IPF. The gene expression profiles associated with these small molecules were often from distinct selections of cell lines, and thus direct connectivity mapping analysis may be susceptible to biological variation introduced by cell lines. In addition, it has been shown that integration of prior knowledge, particularly in the form of gene sets information in biological pathways, has been shown to improve the accuracy of drug activity predictions (26). We evaluated drug-IPF connectivity through enriched pathways directly related to IPF under the assumption that pathways perturbed by drugs are more stable across different host cell conditions compared to individual genes. Annotation-based connectivity analysis lead to discovery of additional 14 small molecules that were not included in the CLUE platform. These include aurora kinase inhibitor barasertib-HQPA and phosphodiesterase inhibitor roflumilast. Notably, nintedanib was also among the 14 additional small molecules, and the enriched pathways that contributed to the connection to IPF were related to fibroblast proliferation, ECM production and cell migration, which is in consistent with implicated MoA of nintedanib against IPF *in vitro* (27).

Among the 77 prioritized candidates, 31 are FDA-approved drugs and are associated with different MoAs. These MoAs include RTK inhibition, which is the known MoA for the approved IPF drug nintedanib. Other compounds with this MoA in our discovered candidate compounds included pazopanib and sunitinib. Sunitinib is approved for treatment of renal cell carcinoma and

gastrointestinal stromal tumor, and it has also been shown to be efficacious in inhibiting established pulmonary fibrosis in the bleomycin-induced mouse model (28). Additionally, MoAs involved with these 31 drugs also included those associated with compounds that are currently investigated or are in clinical trial for IPF drugs, such as src-kinase inhibitor and mTOR inhibitor (29). The MoAs associated with the remaining IPF repositioning candidates included aurora kinase inhibitor, EGFR inhibitor, calcium channel blocker, phosphodiesterase inhibitor, PPAR agonist, Bcr-Abl kinase inhibitors and opioid receptor antagonist.

HDACIs have been reported to improve resolution of pulmonary fibrosis in mice (19, 20). Entinostat (MS-275 or SNDX-275), a class I HDACI is currently investigated (Phase II) for metastatic colorectal cancer (30), breast cancer (31), relapsed and refractory Hodgkin lymphoma (32), and myeloid malignancies (33, 34). These ongoing trials, and our preliminary in vitro data, suggests repositioning potential of entinostat in IPF.

In conclusion, we have developed a generalizable, integrative connectivity analysis combining information from transcriptomic profiles, disease systems biology and drug cheminformatics for *in silico* IPF drug discovery. Application of our approach earlier in the IPF drug discovery pipeline may help to avert late stage clinical trial failures. As almost half the candidates we have discovered in this study are FDA-approved or are currently in clinical trials for a number of diseases, rapid translation of these compounds is feasible. Finally, we have suggested novel drug mechanisms that could shed new insights in the search for better IPF drugs.

Acknowledgements

This study was supported in part by the NIH grants NHLBI 1R21HL133539 and 1R21HL135368 (to AGJ), 1R01 HL134801 (to SKM), US Department of Defense grant W81XWH-17-1-0666 (to SKM) and by the Cincinnati Children's Hospital and Medical Center.

Conflicts of interest

The authors declare no conflicts of interest.

Author contributions

Y.W. and A.J. conceived this study. Y.W., J.Y., and S.G. collected and analyzed data. Y.W. and A.J. interpreted results from data. T.C. and S.M. conducted experimental validations. Y.W, S.M., and A.J edited this manuscript. Y.W. wrote the first draft.

Tables

Table 1: Summary of 6 datasets comparing IPF lung tissue with healthy controls.

GEO Data set	Sample description	Reference
GSE10667	23 IPF samples and 16 controls	(35, 36)
GSE24206	17 IPF samples and 6 controls	(37)
GSE48149	13 IPF samples and 9 controls	(38)
GSE53845	40 IPF samples and 8 controls	(22)
GSE47460	131 IPF samples and 12 controls	LGRC
GSE101286	7 IPF samples and 3 controls	(39)

Table 2: List of 39 potential repurposing candidates for IPF.

Compound	IPF-related MOA	Indication	Phase
febuxostat	xanthine oxidase inhibitor	hyperuricemia	Launched
nortriptyline	tricyclic antidepressant	depression	Launched
amsacrine	topoisomerase inhibitor	cancer	Launched
irinotecan	topoisomerase inhibitor	cancer	Launched
camptothecin	topoisomerase inhibitor	cancer	Phase 3
pioglitazone	ppar receptor agonist, insulin sensitizer	diabetes mellitus	Launched
roflumilast	phosphodiesterase inhibitor	COPD	Launched
sildenafil	phosphodiesterase inhibitor	hypertension	Launched
nalbuphine	opioid receptor antagonist	pain relief	Launched
everolimus	mTOR inhibitor	cancer	Launched
sunitinib	mRTK inhibitor	cancer	Launched
nintedanib	mRTK inhibitor	IPF	Launched
dovitinib	mRTK inhibitor	cancer	Phase 3
pazopanib	mRTK inhibitor	cancer	Launched
selegiline	monoamine oxidase inhibitor	Parkinson's Disease	Launched
selumetinib	mek inhibitor	cancer	Phase 3

curcumin	lipoxygenase inhibitor, histone acetyltransferase inhibitor, cyclooxygenase inhibitor		Launched
tomelukast	leukotriene receptor antagonist	asthma	Phase 3
dasatinib	mRTK inhibitor	cancer	Launched
lafutidine	histamine receptor antagonist	duodenal ulcer disease, peptic ulcer disease (PUD)	Launched
ranitidine	histamine receptor antagonist	heartburn	Launched
amodiaquine	histamine receptor agonist	malaria	Launched
entinostat	hdac inhibitor	cancer	Phase 3
remacemide	glutamate receptor antagonist	epilepsy and neurodegenerative diseases	Phase 3
riluzole	glutamate inhibitor	amyotrophic lateral sclerosis (ALS)	Launched
erlotinib	egfr inhibitor	cancer	Launched
gefitinib	egfr inhibitor	cancer	Launched
sulpiride	dopamine receptor antagonist	schizophrenia	Launched
mycophenolic-acid	dehydrogenase inhibitor, inositol monophosphatase inhibitor	organ rejection	Launched
ketorolac	cyclooxygenase inhibitor	NSAID	Launched
mestinon	cholinesterase inhibitor	myasthenia gravis	Launched
fipronil	chloride channel blocker	insecticide	Launched
verapamil	calcium channel blocker	hypertension	Launched
gaboxadol	benzodiazepine receptor agonist	insomnia	Phase 3
ivermectin	benzodiazepine receptor agonist	gastrointestinal parasites	Launched
nilotinib	bcr-abl kinase inhibitor	cancer	Launched
barasertib-HQPA	aurora kinase inhibitor	cancer	Phase 2/Phase 3
regadenoson	adenosine receptor agonist	myocardial perfusion imaging (MPI)	Launched
bucladesine	adenosine receptor agonist	skin ulcer	Launched

Figure legends

Figure 1. Overview of expression and annotation-based connectivity analysis workflow. Works in this study could be summarized in three steps. a) Collection and differential analysis of human IPF datasets; b) Expression-based connectivity analysis through CLUE; c) annotation-based connectivity analysis examining similarity between pathways perturbed by compound and those involved in IPF.

Figure 2. Heat map view of differentially expressed genes in 6 IPF datasets. Expression of 2206 genes unambiguously differentially expressed in at least two IPF dataset were shown. Genes were represented in rows and patient sample were represented in columns. Cells in heat map were sorted discerningly based on median log fold change in 6 datasets and on number of datasets they were differentially expressed in. b) Genes that were up-regulated in at least 4 datasets. Intersection with all known pulmonary fibrosis genes are shown in the Venn graph. 3) Overview of all 6 gene queries made to the CLUE platform. Each query contains 150 up-regulated genes (red) and 150 down-regulated (green) genes.

Figure 3. Gene expression based connectivity score of CLUE compounds. Scatter plot of positive connectivity score against negative connectivity score between each CLUE compound and each IPF dataset across all cell lines. Coordinates of each point were determined by the average of highest or lowest 6 connectivity scores among all 54 values across 6 IPF datasets and 9 cell lines in CLUE. b) Heatmap of connectivity score of 82 compound that were significantly connected to IPF based on permutation analysis.

Figure 4. Enriched pathway heat map view of 345 drugs significantly connected to IPF in annotation-based connectivity analysis. Enrichment terms in categories including KEGG pathways, Wiki pathways, Reactome, Mouse phenotype and Gene Ontology: Biological process enriched in either consistently up-regulated or down-regulated IPF genes are arranged in rows. LINCS drug profiles were arranged in columns. Blue indicates annotation terms are enriched in down-regulated genes by drug or IPF, and yellow indicates annotation terms are enriched in up-regulated genes by drug or IPF. K-means clustering was used to identify compound modules.

Figure 5. Heat map view of candidate compound targets that are differentially expressed in IPF. Log fold changes of 48 target genes of 30 compounds in IPF are shown. Only compounds with targets differentially expressed in at least two IPF datasets are included. Differentially expressed drug targets are in rows and IPF candidate compounds are in columns. Rows and columns are ordered using 2D hierarchical clustering.

Figure 6. Entinostat treatment attenuates pro-fibrotic gene expression. Fibrotic lungs of TGFα mice on Dox for four weeks were cultured to isolate primary lung fibroblasts and treated with either vehicle or entinostat (MS 275; 1 μM) for 16 hrs or 48 hrs. (A) Total RNA was analyzed for the expression of fibroproliferative genes, CCNA2 and CCNB2 using RT-PCR. (B) Total RNA was analyzed for the expression of αSMA and KIF20A using RT-PCR. ***P<0.0005; ****P<0.00005.

References

1. Kekevian A, Gershwin ME, Chang C. Diagnosis and classification of idiopathic pulmonary fibrosis. *Autoimmun Rev* 2014; 13: 508-512.
2. Raghu G, Collard HR, Egan JJ, Martinez FJ, Behr J, Brown KK, Colby TV, Cordier JF, Flaherty KR, Lasky JA, Lynch DA, Ryu JH, Swigris JJ, Wells AU, Ancochea J, Bouros D, Carvalho C, Costabel U, Ebina M, Hansell DM, Johkoh T, Kim DS, King TE, Jr., Kondoh Y, Myers J, Muller NL, Nicholson AG, Richeldi L, Selman M, Dudden RF, Griss BS, Protzko SL, Schunemann HJ, Fibrosis AEJACoIP. An official ATS/ERS/JRS/ALAT statement: idiopathic pulmonary fibrosis: evidence-based guidelines for diagnosis and management. *Am J Respir Crit Care Med* 2011; 183: 788-824.
3. Richeldi L, du Bois RM, Raghu G, Azuma A, Brown KK, Costabel U, Cottin V, Flaherty KR, Hansell DM, Inoue Y, Kim DS, Kolb M, Nicholson AG, Noble PW, Selman M, Taniguchi H, Brun M, Le Maulf F, Girard M, Stowasser S, Schlenker-Herceg R, Disse B, Collard HR, Investigators IT. Efficacy and safety of nintedanib in idiopathic pulmonary fibrosis. *The New England journal of medicine* 2014; 370: 2071-2082.
4. King TE, Jr., Bradford WZ, Castro-Bernardini S, Fagan EA, Glaspole I, Glassberg MK, Gorina E, Hopkins PM, Kardatzke D, Lancaster L, Lederer DJ, Nathan SD, Pereira CA, Sahn SA, Sussman R, Swigris JJ, Noble PW, Group AS. A phase 3 trial of pirfenidone in patients with idiopathic pulmonary fibrosis. *The New England journal of medicine* 2014; 370: 2083-2092.
5. Margolis R, Derr L, Dunn M, Huerta M, Larkin J, Sheehan J, Guyer M, Green ED. The National Institutes of Health's Big Data to Knowledge (BD2K) initiative: capitalizing on biomedical big data. *J Am Med Inform Assoc* 2014; 21: 957-958.
6. Barrett T, Wilhite SE, Ledoux P, Evangelista C, Kim IF, Tomashevsky M, Marshall KA, Phillippy KH, Sherman PM, Holko M, Yefanov A, Lee H, Zhang N, Robertson CL, Serova N, Davis S, Soboleva A. NCBI GEO: archive for functional genomics data sets--update. *Nucleic Acids Res* 2013; 41: D991-995.
7. Szklarczyk D, Morris JH, Cook H, Kuhn M, Wyder S, Simonovic M, Santos A, Doncheva NT, Roth A, Bork P, Jensen LJ, von Mering C. The STRING database in 2017: quality-controlled protein-protein association networks, made broadly accessible. *Nucleic Acids Res* 2017; 45: D362-D368.
8. Subramanian A, Narayan R, Corsello SM, Peck DD, Natoli TE, Lu X, Gould J, Davis JF, Tubelli AA, Asiedu JK, Lahr DL, Hirschman JE, Liu Z, Donahue M, Julian B, Khan M, Wadden D, Smith IC, Lam D, Liberzon A, Toder C, Bagul M, Orzechowski M, Enache OM, Piccioni F, Johnson SA, Lyons NJ, Berger AH, Shamji AF, Brooks AN, Vrcic A, Flynn C, Rosains J, Takeda DY, Hu R, Davison D, Lamb J, Ardlie K, Hogstrom L, Greenside P, Gray NS, Clemons PA, Silver S, Wu X, Zhao WN, Read-Button W, Wu X, Haggarty SJ, Ronco LV, Boehm JS, Schreiber SL, Doench JG, Bittker JA, Root DE, Wong B, Golub TR. A Next Generation Connectivity Map: L1000 Platform and the First 1,000,000 Profiles. *Cell* 2017; 171: 1437-1452 e1417.
9. Lamb J, Ramaswamy S, Ford HL, Contreras B, Martinez RV, Kittrell FS, Zahnow CA, Patterson N, Golub TR, Ewen ME. A mechanism of cyclin D1 action encoded in the patterns of gene expression in human cancer. *Cell* 2003; 114: 323-334.
10. Gerald KB. Nonparametric statistical methods. *Nurse Anesth* 1991; 2: 93-95.

11. Lamb J, Crawford ED, Peck D, Modell JW, Blat IC, Wrobel MJ, Lerner J, Brunet JP, Subramanian A, Ross KN, Reich M, Hieronymus H, Wei G, Armstrong SA, Haggarty SJ, Clemons PA, Wei R, Carr SA, Lander ES, Golub TR. The Connectivity Map: using gene-expression signatures to connect small molecules, genes, and disease. *Science* 2006; 313: 1929-1935.
12. Qu XA, Rajpal DK. Applications of Connectivity Map in drug discovery and development. *Drug Discov Today* 2012; 17: 1289-1298.
13. Wang Y, Arora K, Yang F, Shin W-H, Chen J, Kihara D, Naren AP, Jegga AG. PP-2, a src-kinase inhibitor, is a potential corrector for F508del-CFTR in cystic fibrosis. *bioRxiv* 2018.
14. Sontake V, Wang Y, Kasam RK, Sinner D, Reddy GB, Naren AP, McCormack FX, White ES, Jegga AG, Madala SK. Hsp90 regulation of fibroblast activation in pulmonary fibrosis. *JCI Insight* 2017; 2: e91454.
15. Iorio F, Bosotti R, Scacheri E, Belcastro V, Mithbaokar P, Ferriero R, Murino L, Tagliaferri R, Brunetti-Pierri N, Isacchi A, di Bernardo D. Discovery of drug mode of action and drug repositioning from transcriptional responses. *Proc Natl Acad Sci U S A* 2010; 107: 14621-14626.
16. Iorio F, Isacchi A, di Bernardo D, Brunetti-Pierri N. Identification of small molecules enhancing autophagic function from drug network analysis. *Autophagy* 2010; 6: 1204-1205.
17. Karatzas E, Bourdakou MM, Kolios G, Spyrou GM. Drug repurposing in idiopathic pulmonary fibrosis filtered by a bioinformatics-derived composite score. *Sci Rep* 2017; 7: 12569.
18. Peyvandipour A, Saberian N, Shafi A, Donato M, Draghici S. A novel computational approach for drug repurposing using systems biology. *Bioinformatics* 2018; 34: 2817-2825.
19. Saito S, Zhuang Y, Suzuki T, Ota Y, Bateman ME, Alkhatib AL, Morris GF, Lasky JA. HDAC8 inhibition ameliorates pulmonary fibrosis. *Am J Physiol Lung Cell Mol Physiol* 2019; 316: L175-L186.
20. Sanders YY, Hagood JS, Liu H, Zhang W, Ambalavanan N, Thannickal VJ. Histone deacetylase inhibition promotes fibroblast apoptosis and ameliorates pulmonary fibrosis in mice. *Eur Respir J* 2014; 43: 1448-1458.
21. Barrett T, Troup DB, Wilhite SE, Ledoux P, Rudnev D, Evangelista C, Kim IF, Soboleva A, Tomashevsky M, Edgar R. NCBI GEO: mining tens of millions of expression profiles--database and tools update. *Nucleic Acids Res* 2007; 35: D760-765.
22. DePianto DJ, Chandriani S, Abbas AR, Jia G, N'Diaye EN, Caplazi P, Kauder SE, Biswas S, Karnik SK, Ha C, Modrusan Z, Matthay MA, Kukreja J, Collard HR, Egen JG, Wolters PJ, Arron JR. Heterogeneous gene expression signatures correspond to distinct lung pathologies and biomarkers of disease severity in idiopathic pulmonary fibrosis. *Thorax* 2015; 70: 48-56.
23. Wang Y, Yella J, Chen J, McCormack FX, Madala SK, Jegga AG. Unsupervised gene expression analyses identify IPF-severity correlated signatures, associated genes and biomarkers. *BMC Pulm Med* 2017; 17: 133.
24. Ritchie ME, Phipson B, Wu D, Hu YF, Law CW, Shi W, Smyth GK. limma powers differential expression analyses for RNA-sequencing and microarray studies. *Nucleic Acids Research* 2015; 43.

25. Chen J, Bardes EE, Aronow BJ, Jegga AG. ToppGene Suite for gene list enrichment analysis and candidate gene prioritization. *Nucleic Acids Res* 2009; 37: W305-311.
26. Costello JC, Heiser LM, Georgii E, Gonen M, Menden MP, Wang NJ, Bansal M, Ammad-ud-din M, Hintsanen P, Khan SA, Mpindi JP, Kallioniemi O, Honkela A, Aittokallio T, Wennerberg K, Community ND, Collins JJ, Gallahan D, Singer D, Saez-Rodriguez J, Kaski S, Gray JW, Stolovitzky G. A community effort to assess and improve drug sensitivity prediction algorithms. *Nat Biotechnol* 2014; 32: 1202-1212.
27. Wollin L, Wex E, Pautsch A, Schnapp G, Hostettler KE, Stowasser S, Kolb M. Mode of action of nintedanib in the treatment of idiopathic pulmonary fibrosis. *Eur Respir J* 2015; 45: 1434-1445.
28. Huang X, Wang W, Yuan H, Sun J, Li L, Wu X, Luo J, Gu Y. Sunitinib, a Small-Molecule Kinase Inhibitor, Attenuates Bleomycin-Induced Pulmonary Fibrosis in Mice. *Tohoku J Exp Med* 2016; 239: 251-261.
29. Raghu G, Behr J, Brown KK, Egan JJ, Kawut SM, Flaherty KR, Martinez FJ, Nathan SD, Wells AU, Collard HR, Costabel U, Richeldi L, de Andrade J, Khalil N, Morrison LD, Lederer DJ, Shao L, Li X, Pedersen PS, Montgomery AB, Chien JW, O'Riordan TG, Investigators* A-I. Treatment of idiopathic pulmonary fibrosis with ambrisentan: a parallel, randomized trial. *Ann Intern Med* 2013; 158: 641-649.
30. Azad NS, El-Khoueiry A, Yin J, Oberg AL, Flynn P, Adkins D, Sharma A, Weisenberger DJ, Brown T, Medvari P, Jones PA, Easwaran H, Kamel I, Bahary N, Kim G, Picus J, Pitot HC, Erlichman C, Donehower R, Shen H, Laird PW, Piekarz R, Baylin S, Ahuja N. Combination epigenetic therapy in metastatic colorectal cancer (mCRC) with subcutaneous 5-azacitidine and entinostat: a phase 2 consortium/stand up 2 cancer study. *Oncotarget* 2017; 8: 35326-35338.
31. Connolly RM, Li H, Jankowitz RC, Zhang Z, Rudek MA, Jeter SC, Slater SA, Powers P, Wolff AC, Fetting JH, Brufsky A, Piekarz R, Ahuja N, Laird PW, Shen H, Weisenberger DJ, Cope L, Herman JG, Somlo G, Garcia AA, Jones PA, Baylin SB, Davidson NE, Zahnow CA, Stearns V. Combination Epigenetic Therapy in Advanced Breast Cancer with 5-Azacitidine and Entinostat: A Phase II National Cancer Institute/Stand Up to Cancer Study. *Clin Cancer Res* 2017; 23: 2691-2701.
32. Batlevi CL, Kasamon Y, Bociek RG, Lee P, Gore L, Copeland A, Sorensen R, Ordentlich P, Cruickshank S, Kunkel L, Buglio D, Hernandez-Ilizaliturri F, Younes A. ENGAGE- 501: phase II study of entinostat (SNDX-275) in relapsed and refractory Hodgkin lymphoma. *Haematologica* 2016; 101: 968-975.
33. Prebet T, Sun Z, Ketterling RP, Zeidan A, Greenberg P, Herman J, Juckett M, Smith MR, Malick L, Paietta E, Czader M, Figueroa M, Gabrilove J, Erba HP, Tallman MS, Litzow M, Gore SD, Eastern Cooperative Oncology G, North American Leukemia i. Azacitidine with or without Entinostat for the treatment of therapy-related myeloid neoplasm: further results of the E1905 North American Leukemia Intergroup study. *Br J Haematol* 2016; 172: 384-391.
34. Fandy TE, Herman JG, Kerns P, Jiemjit A, Sugar EA, Choi SH, Yang AS, Aucott T, Dauses T, Odchimar-Reissig R, Licht J, McConnell MJ, Nasrallah C, Kim MK, Zhang W, Sun Y, Murgo A, Espinoza-Delgado I, Oteiza K, Owoeye I, Silverman LR, Gore SD, Carraway HE. Early epigenetic changes and DNA damage do not predict clinical response in an overlapping schedule of 5-azacytidine and entinostat in patients with myeloid malignancies. *Blood* 2009; 114: 2764-2773.

35. Konishi K, Gibson KF, Lindell KO, Richards TJ, Zhang Y, Dhir R, Bisceglia M, Gilbert S, Yousem SA, Song JW, Kim DS, Kaminski N. Gene expression profiles of acute exacerbations of idiopathic pulmonary fibrosis. *Am J Respir Crit Care Med* 2009; 180: 167-175.
36. Rosas IO, Richards TJ, Konishi K, Zhang Y, Gibson K, Lokshin AE, Lindell KO, Cisneros J, Macdonald SD, Pardo A, Sciurba F, Dauber J, Selman M, Gochuico BR, Kaminski N. MMP1 and MMP7 as potential peripheral blood biomarkers in idiopathic pulmonary fibrosis. *PLoS Med* 2008; 5: e93.
37. Meltzer EB, Barry WT, D'Amico TA, Davis RD, Lin SS, Onaitis MW, Morrison LD, Sporn TA, Steele MP, Noble PW. Bayesian probit regression model for the diagnosis of pulmonary fibrosis: proof-of-principle. *BMC Med Genomics* 2011; 4: 70.
38. Hsu E, Shi H, Jordan RM, Lyons-Weiler J, Pilewski JM, Feghali-Bostwick CA. Lung tissues in patients with systemic sclerosis have gene expression patterns unique to pulmonary fibrosis and pulmonary hypertension. *Arthritis Rheum* 2011; 63: 783-794.
39. Horimasu Y, Ishikawa N, Taniwaki M, Yamaguchi K, Hamai K, Iwamoto H, Ohshimo S, Hamada H, Hattori N, Okada M, Arihiro K, Ohtsuki Y, Kohno N. Gene expression profiling of idiopathic interstitial pneumonias (IIPs): identification of potential diagnostic markers and therapeutic targets. *BMC Med Genet* 2017; 18: 88.

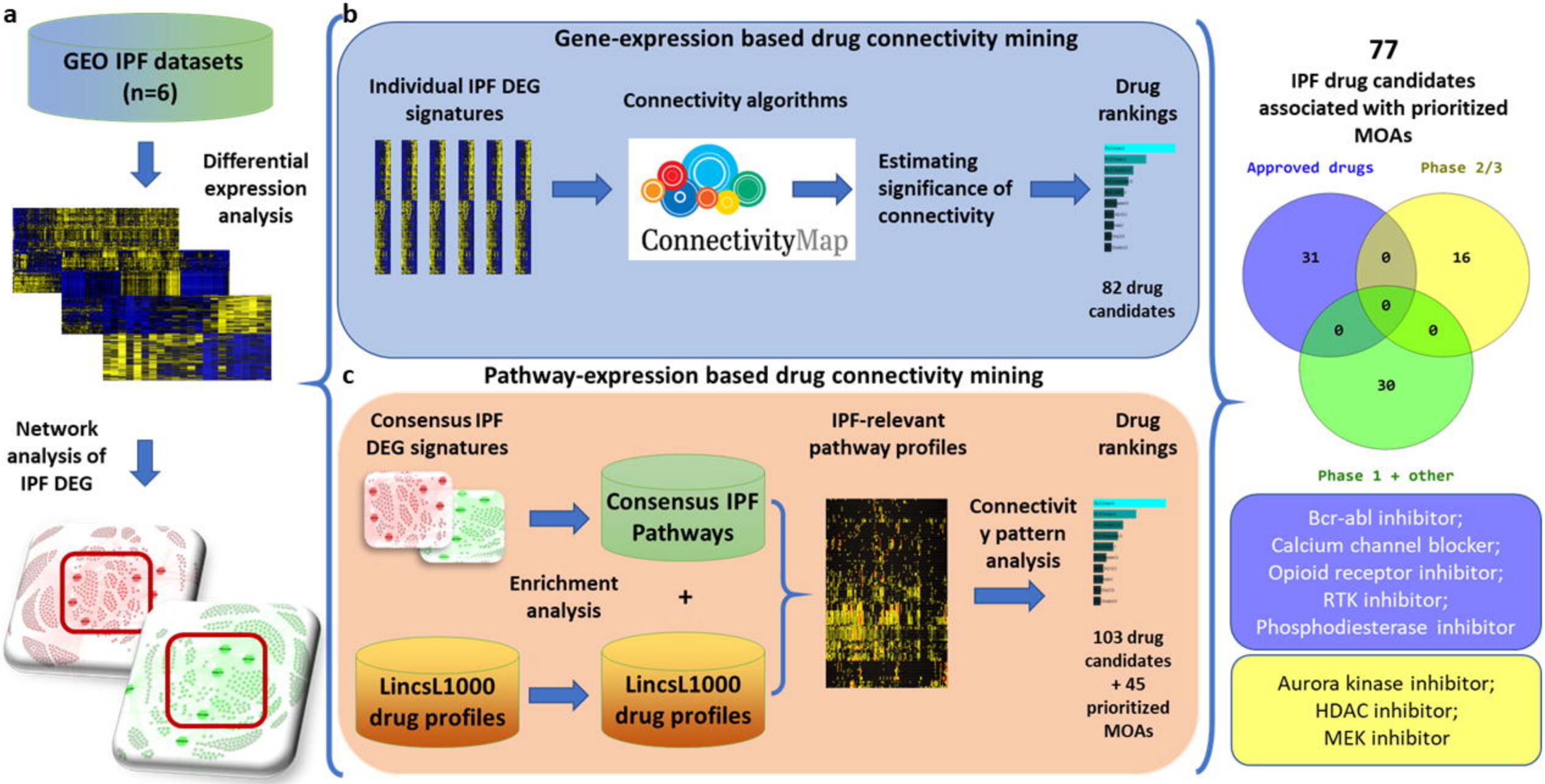
a
GEO IPF datasets (n=6)
Differential expression analysis
Network analysis of IPF DEG
b
Gene-expression based drug connectivity mining
Individual IPF DEG signatures
Connectivity algorithms
ConnectivityMap
Estimating significance of connectivity
Drug rankings
82 drug candidates
c
Pathway-expression based drug connectivity mining
Consensus IPF DEG signatures
Consensus IPF Pathways
Enrichment analysis
+
LincsL1000 drug profiles
LincsL1000 drug profiles
IPF-relevant pathway profiles
Connectivity pattern analysis
Drug rankings
103 drug candidates + 45 prioritized MOAs
77
IPF drug candidates associated with prioritized MOAs
Approved drugs
Phase 2/3
Phase 1 + other
31
0
16
0
0
0
30
Bcr-abl inhibitor;
Calcium channel blocker;
Opioid receptor inhibitor;
RTK inhibitor;
Phosphodiesterase inhibitor
Aurora kinase inhibitor;
HDAC inhibitor;
MEK inhibitor

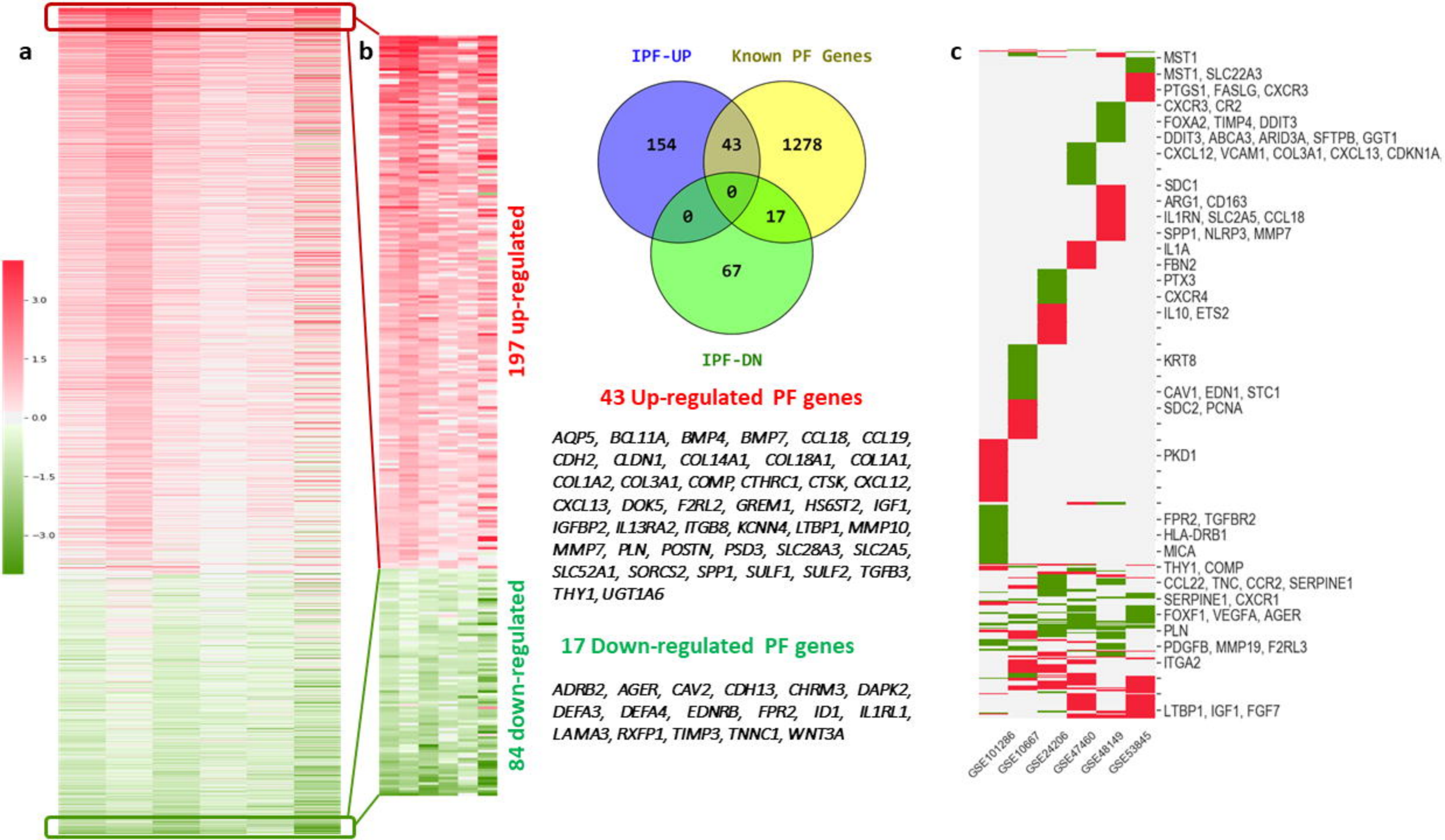
a
b
3.0
1.5
0.0
−1.5
−3.0
197 up-regulated
84 down-regulated
IPF-UP
Known PF Genes
IPF-DN
154
43
1278
0
0
17
67
43 Up-regulated PF genes
AQP5, BCL11A, BMP4, BMP7, CCL18, CCL19, CDH2, CLDN1, COL14A1, COL18A1, COL1A1, COL1A2, COL3A1, COMP, CTHRC1, CTSK, CXCL12, CXCL13, DOK5, F2RL2, GREM1, HS6ST2, IGF1, IGFBP2, IL13RA2, ITGB8, KCNN4, LTBP1, MMP10, MMP7, PLN, POSTN, PSD3, SLC28A3, SLC2A5, SLC52A1, SORCS2, SPP1, SULF1, SULF2, TGFB3, THY1, UGT1A6
17 Down-regulated PF genes
ADRB2, AGER, CAV2, CDH13, CHRM3, DAPK2, DEFA3, DEFA4, EDNRB, FPR2, ID1, IL1RL1, LAMA3, RXFP1, TIMP3, TNNC1, WNT3A
c
MST1
MST1, SLC22A3
PTGS1, FASLG, CXCR3
CXCR3, CR2
FOXA2, TIMP4, DDIT3
DDIT3, ABCA3, ARID3A, SFTPB, GGT1
CXCL12, VCAM1, COL3A1, CXCL13, CDKN1A
SDC1
ARG1, CD163
IL1RN, SLC2A5, CCL18
SPP1, NLRP3, MMP7
IL1A
FBN2
PTX3
CXCR4
IL10, ETS2
KRT8
CAV1, EDN1, STC1
SDC2, PCNA
PKD1
FPR2, TGFBR2
HLA-DRB1
MICA
THY1, COMP
CCL22, TNC, CCR2, SERPINE1
SERPINE1, CXCR1
FOXF1, VEGFA, AGER
PLN
PDGFB, MMP19, F2RL3
ITGA2
LTBP1, IGF1, FGF7
GSE101286
GSE10667
GSE24206
GSE47460
GSE48149
GSE53845

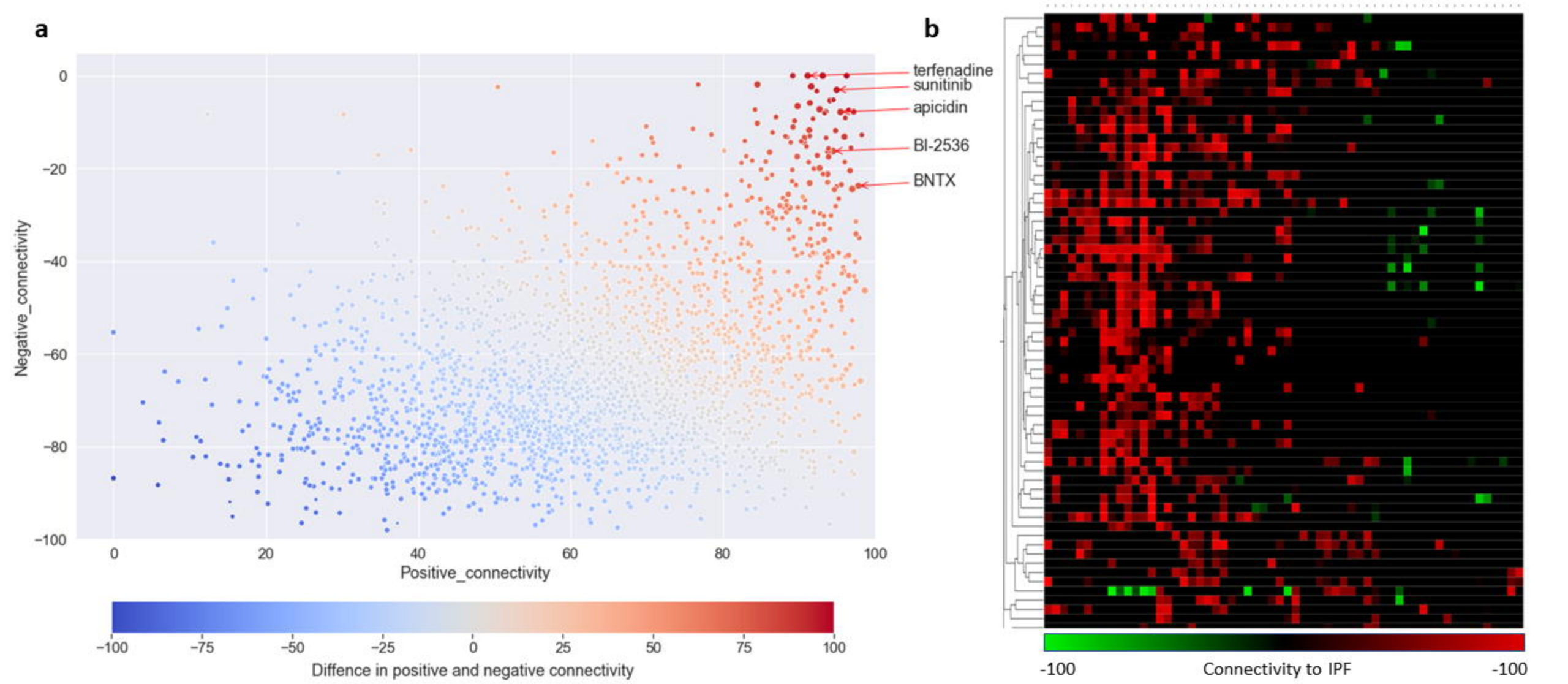
a
b
terfenadine
sunitinib
apicidin
BI-2536
BNTX
Negative_connectivity
Positive_connectivity
0
−20
−40
−60
−80
−100
0
20
40
60
80
100
−100
−75
−50
−25
0
25
50
75
100
Diffence in positive and negative connectivity
-100
Connectivity to IPF
-100

IVERMECTIN
PAZOPANIB
ERLOTINIB
NINTEDANIB
NVP-AUY922
SILDENAFIL
ADATANSERIN

MLN-8054
DASATINIB
LONAFARNIB
SB-939
GELDANAMYCIN
CMPD-1

BARASERTIB-HQPA
AURORA-A-INHIBITOR-I
NILOTINIB
GABOXADOL
PAZOPANIB
GEFITINIB
DOVITINIB
WZ-4002
IKK-16
SB-239063
ROFLUMILAST
VOLASERTIB
NVP-TAE226
SB-221284
COMBRETASTATIN-A-4

PALOMID-529
PCI-34051
RANITIDINE
ADATANSERIN

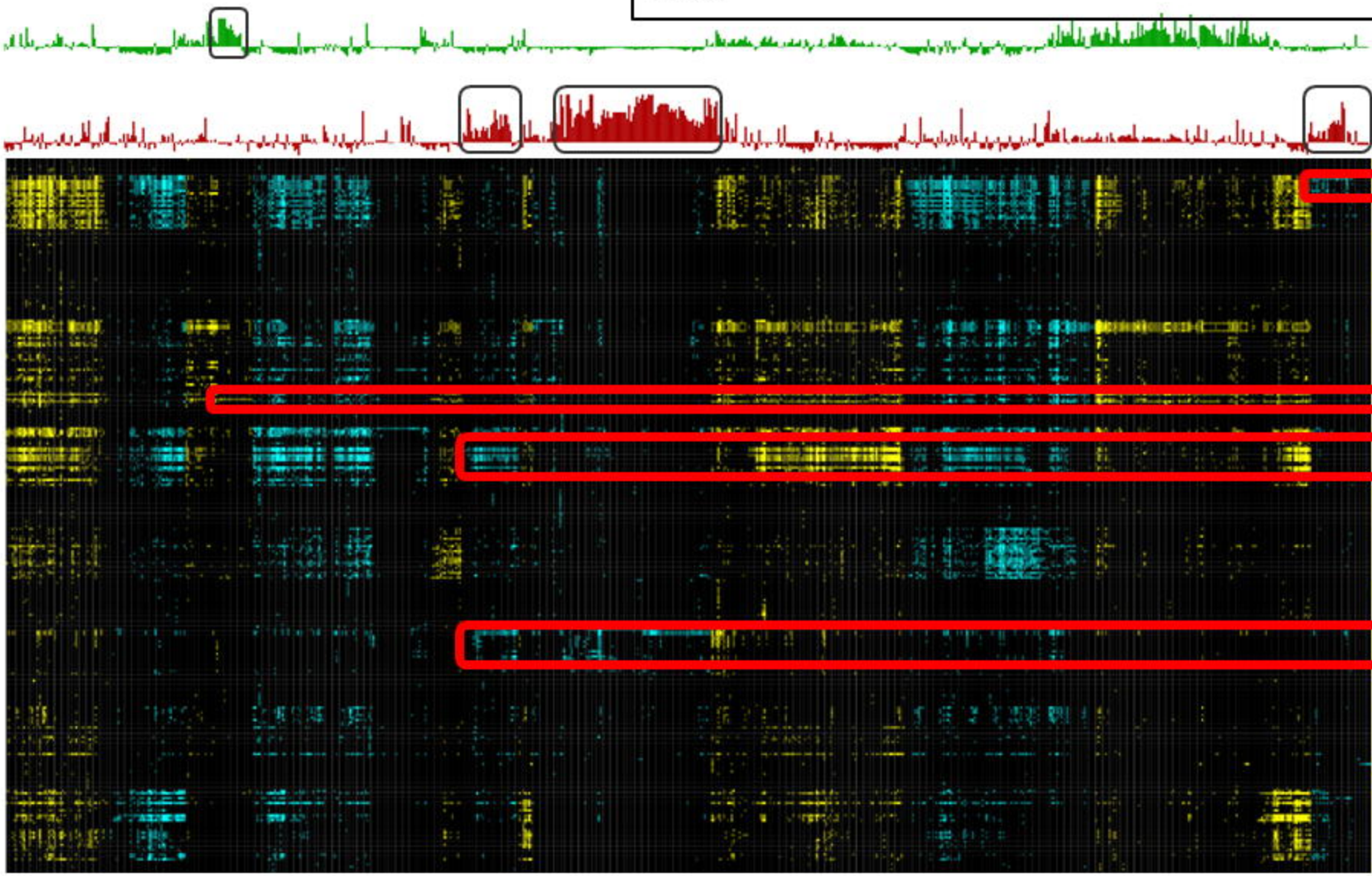

cell migration;
cell motility;
regulation of cell adhesion

blood vessel morphogenesis;
anatomical structure formation involved in morphogenesis;
angiogenesis

programmed cell death;
regulation of programmed cell death

collagen metabolic process;
Collagen chain trimerization;
Collagen biosynthesis and modifying enzymes;
Protein digestion and absorption;
collagen fibril organization

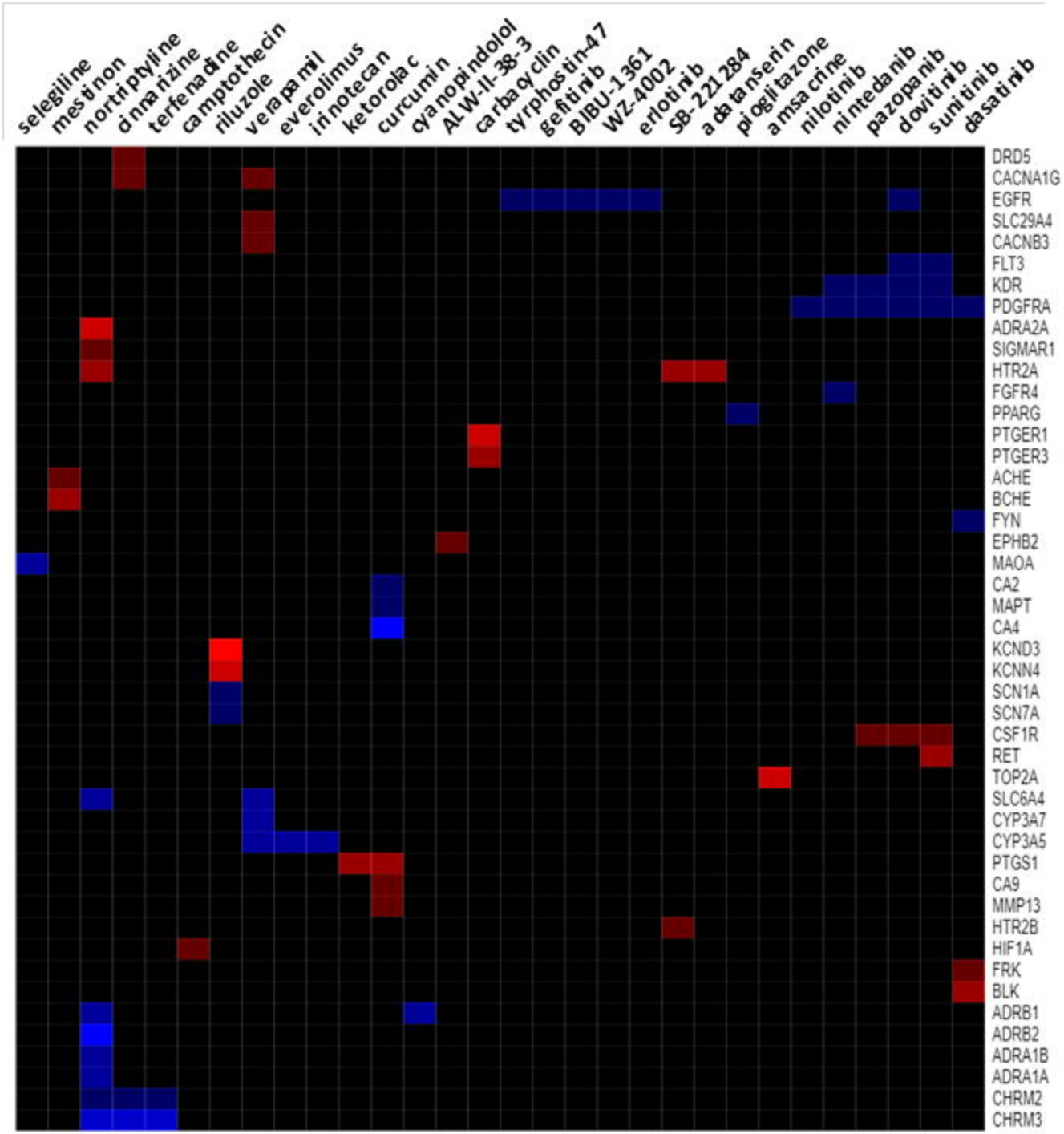
selegiline
mestinon
nortriptyline
cinnarizine
terfenadine
camptothecin
riluzole
verapamil
everolimus
irinotecan
ketorolac
curcumin
cyanopindolol
ALW-II-38-3
carbacyclin
tyrphostin-47
gefitinib
BIBU-1361
WZ-4002
erlotinib
SB-221284
adatanserin
pioglitazone
amsacrine
nilotinib
nintedanib
pazopanib
dovitinib
sunitinib
dasatinib
DRD5
CACNA1G
EGFR
SLC29A4
CACNB3
FLT3
KDR
PDGFRA
ADRA2A
SIGMAR1
HTR2A
FGFR4
PPARG
PTGER1
PTGER3
ACHE
BCHE
FYN
EPHB2
MAOA
CA2
MAPT
CA4
KCND3
KCNN4
SCN1A
SCN7A
CSF1R
RET
TOP2A
SLC6A4
CYP3A7
CYP3A5
PTGS1
CA9
MMP13
HTR2B
HIF1A
FRK
BLK
ADRB1
ADRB2
ADRA1B
ADRA1A
CHRM2
CHRM3

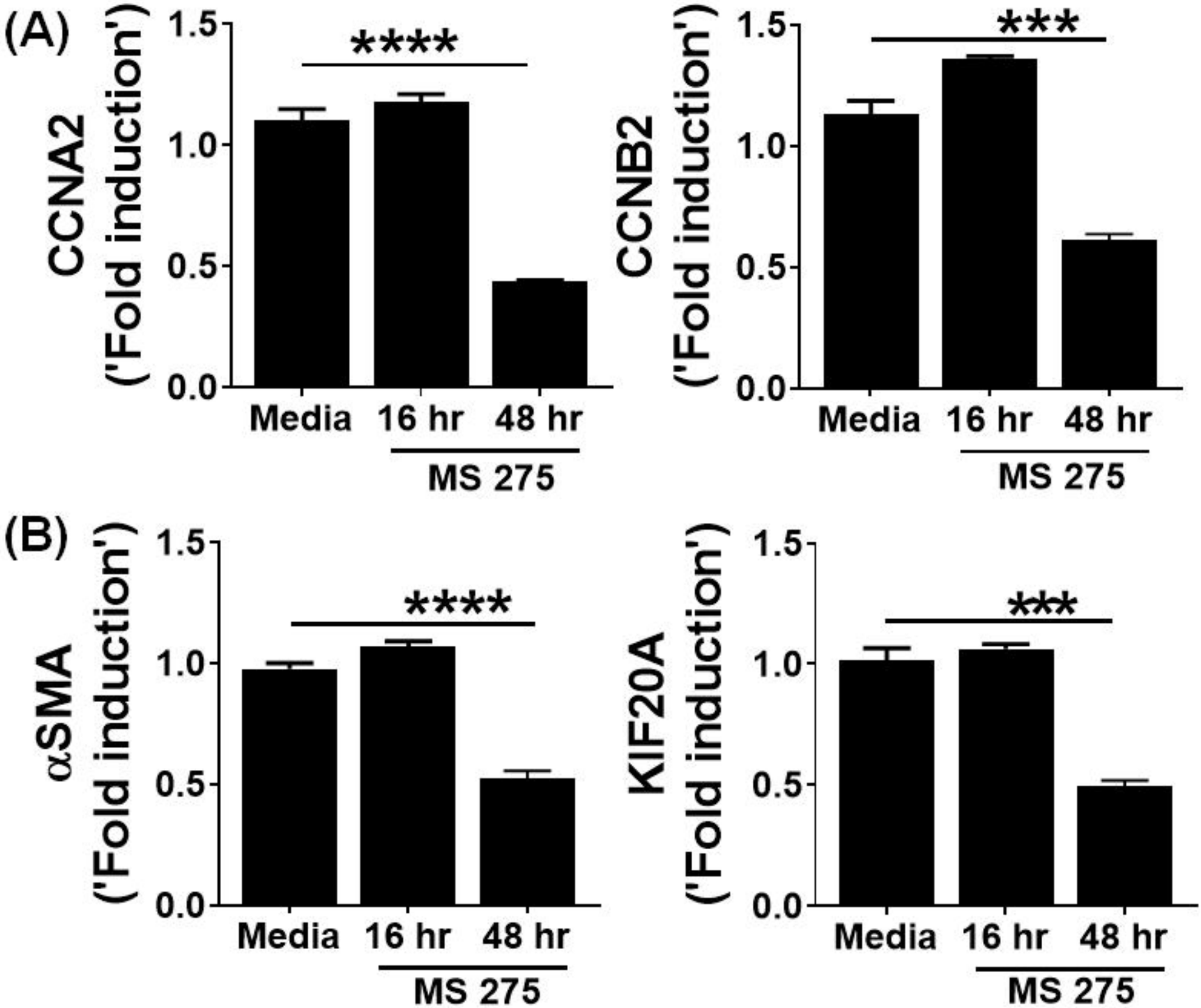
(A)
CCNA2
('Fold induction')
1.5
1.0
0.5
0.0
****
Media
16 hr
48 hr
MS 275
CCNB2
('Fold induction')
1.5
1.0
0.5
0.0
***
Media
16 hr
48 hr
MS 275
(B)
αSMA
('Fold induction')
1.5
1.0
0.5
0.0
****
Media
16 hr
48 hr
MS 275
KIF20A
('Fold induction')
1.5
1.0
0.5
0.0
***
Media
16 hr
48 hr
MS 275